

**This item is the archived peer-reviewed author-version of:**

Empowering a mesophilic inoculum for thermophilic nitrification : growth mode and temperature pattern as critical proliferation factors for archaeal ammonia oxidizers

**Reference:**

Courtens Emilie N.P., Vandekerckhove Tom, Prat Delphine, Vilchez-Vargas Ramiro, Vital Marius, Pieper Dietmar H., Meerbergen Ken, Lievens Bart, Boon Nico, Vlaeminck Siegfried.- Empowering a mesophilic inoculum for thermophilic nitrification : growth mode and temperature pattern as critical proliferation factors for archaeal ammonia oxidizers  
Water research / International Association on Water Pollution Research - ISSN 0043-1354 - 92(2016), p. 94-103

Full text (Publishers DOI): <http://dx.doi.org/doi:10.1016/j.watres.2016.01.022>

To cite this reference: <http://hdl.handle.net/10067/1304440151162165141>

1 **Empowering a mesophilic inoculum for thermophilic nitrification: growth mode and**  
2 **temperature pattern as critical proliferation factors for archaeal ammonia oxidizers**

3

4 Emilie N. P. Courtens<sup>1</sup>, Tom Vandekerckhove<sup>1</sup>, Delphine Prat<sup>1</sup>, Ramiro Vilchez-Vargas<sup>1</sup>,  
5 Marius Vital<sup>2</sup>, Dietmar H. Pieper<sup>2</sup>, Ken Meerbergen<sup>3</sup>, Bart Lievens<sup>3</sup>, Nico Boon<sup>1\*</sup> and  
6 Siegfried E. Vlaeminck<sup>1,4,\*</sup>✉

7

8 <sup>1</sup>Laboratory of Microbial Ecology and Technology (LabMET), Ghent University, Coupure Links 653, 9000  
9 Gent, Belgium

10 <sup>2</sup>Microbial Interactions and Processes Research Group, Helmholtz Centre for Infection Research, Braunschweig,  
11 Germany

12 <sup>3</sup>Laboratory for Process Microbial Ecology and Bioinspirational Management (PME&BIM), KU Leuven,  
13 Campus De Nayer, Fortsesteenweg 30A, 2860 Sint-Katelijne-Waver, Belgium

14 <sup>4</sup>Research Group of Sustainable Energy, Air and Water Technology, Department of Bioscience Engineering,  
15 University of Antwerp, Groenenborgerlaan 171, 2020 Antwerpen, Belgium

16

17 \*These authors contributed equally and are both senior authors for this work

18 ✉ Corresponding author: Siegfried E. Vlaeminck

19 Tel.: +32-9-2645976

20 Fax: +32-9-2646248

21 E-mail: [siegfried.vlaeminck@UGent.be](mailto:siegfried.vlaeminck@UGent.be)

22

23 **Keywords: Archaea, thermophile, *Nitrospira*, *Nitrososphaera***

24 **Abstract**

25

26 Cost-efficient biological treatment of warm nitrogenous wastewaters requires the  
27 development of thermophilic nitrogen removal processes. Only one thermophilic nitrifying  
28 bioreactor was described so far, achieving  $200 \text{ mg N L}^{-1} \text{ d}^{-1}$  after more than 300 days of  
29 enrichment from compost samples. From the practical point of view in which existing plants  
30 would be upgraded, however, a more time-efficient development strategy based on  
31 mesophilic nitrifying sludge is preferred. This study evaluated the adaptive capacities of  
32 mesophilic nitrifying sludge for two linear temperature increase patterns (non-oscillating vs.  
33 oscillating), two different slopes ( $0.25$  vs.  $0.08 \text{ }^\circ\text{C d}^{-1}$ ) and two different reactor types (floc vs.  
34 biofilm growth). The oscillating temperature pattern ( $0.25 \text{ }^\circ\text{C d}^{-1}$ ) and the moving bed biofilm  
35 reactor ( $0.08 \text{ }^\circ\text{C d}^{-1}$ ) could not reach nitrification at temperatures higher than  $46^\circ\text{C}$ . However,  
36 nitrification rates up to  $800 \text{ mg N L}^{-1} \text{ d}^{-1}$  and  $150 \text{ mg N g}^{-1} \text{ volatile suspended solids d}^{-1}$  were  
37 achieved at a temperature as high as  $49^\circ\text{C}$  by imposing the slowest linear temperature increase  
38 to floccular sludge. Microbial community analysis revealed that this successful transition was  
39 related with a shift in ammonium oxidizing archaea dominating ammonia oxidizing bacteria,  
40 while for nitrite oxidation *Nitrospira* spp. was constantly more abundant than *Nitrobacter*  
41 spp.. This observation was accompanied with an increase in observed sludge yield and a shift  
42 in maximal optimum temperature, determined with ex-situ temperature sensitivity  
43 measurements, predicting an upcoming reactor failure at higher temperature. Overall, this  
44 study achieved nitrification at  $49^\circ\text{C}$  within 150 days by gradual adaptation of mesophilic  
45 sludge, and showed that ex-situ temperature sensitivity screening can be used to monitor and  
46 steer the transition process.

## 47 **1. Introduction**

48 The extensive production of inorganic nitrogen fertilizers is crucial to sustain food production  
49 for the increasing global population and living standard (Erisman et al. 2008). This, however,  
50 resulted in the accumulation of reactive nitrogen species in many natural ecosystems, causing  
51 a worldwide environmental problem (Galloway et al. 2014). Ammonia nitrogen is a major  
52 wastewater component inducing eutrophication and fish mortality when released in water  
53 bodies without prior treatment (Camargo and Alonso 2006). Nitrification, the microbial  
54 oxidation of ammonium to nitrate, plays a key role in the initial transformation of reactive  
55 nitrogen in wastewater treatment. Aerobic ammonium-oxidizing bacteria (AOB) and archaea  
56 (AOA) catalyze the first, rate-limiting step, i.e. oxidation of ammonium ( $\text{NH}_4^+$ ) to nitrite  
57 ( $\text{NO}_2^-$ ) (also known as nitritation), while the successive oxidation to nitrate ( $\text{NO}_3^-$ ) (also  
58 referred to as nitrataion), is usually carried out by aerobic nitrite-oxidizing bacteria (NOB).  
59 Nitrification is conventionally followed by the reductive denitrification process to achieve  
60 complete nitrogen removal, although short-cut nitrogen removal processes, such as partial  
61 nitritation/anammox (PN/A), are gaining importance over the last years (Lackner et al. 2014,  
62 Vlaeminck et al. 2012).

63 Although nitrification is an established biological process to treat ammoniacal wastewater,  
64 applications above 40°C still represent a significant challenge. The development of  
65 thermophilic nitrification could enable the treatment of warm wastewaters, such as hot  
66 industrial wastewater and thermophilic anaerobic digester supernatant, without the need of  
67 additional cooling and thus lower both the capital as operational costs. Experiences with  
68 carbon treatment, moreover, suggest that a more stable process with higher specific rates  
69 (smaller bioreactors), a lower sludge production and a lower level of contamination could be  
70 achieved at thermophilic conditions (Lapara and Alleman 1999). Thermophilic nitrogen

71 removal would, thus, not only be a sustainable and an economically favorable solution for the  
72 treatment of warm wastewaters, but also for wastewaters on sites with excess available heat.

73 Two fundamentally different strategies can be used to achieve thermophilic nitrification for  
74 wastewater treatment, including a strategy based on a thermophilic nitrifying inoculum or  
75 based on a mesophilic community which has been adapted to higher temperatures. As both  
76 thermophilic AOA (e.g. “*Candidatus Nitrosocaldus yellowstonii*”, “*Candidatus*  
77 *Nitrososphaera gargensis*”) and NOB (e.g. *Nitrospira calida*) have been separately enriched  
78 from terrestrial hot springs, respective environmental samples may serve as inoculum to  
79 enrich a thermophilic nitrifying community (de la Torre et al. 2008, Hatzenpichler et al. 2008,  
80 Lebedeva et al. 2011). Indeed, Courtens et al. (*Under review*) recently showed the enrichment  
81 of autotrophic thermophilic nitrifiers from compost samples and the successful operation of a  
82 thermophilic nitrifying bioreactor at 50°C with biotechnological potential. However, the low  
83 growth rate and/or low relative abundance of those thermophilic autotrophs in environmental  
84 samples may result in very long and laborious enrichment processes, which may impede the  
85 upgrade of existing wastewater treatment plants. From a practical point of view the second  
86 strategy, in which existing mesophilic nitrifying communities are adapted to elevated  
87 temperatures, may thus be more appropriate. Shore et al. (2012) achieved complete  
88 nitrification at 40°C applying a stepwise temperature increase from 30 to 40°C (10°C d<sup>-1</sup>) to a  
89 moving bed biofilm reactor (MBBR). In a parallel MBBR the temperature was increased from  
90 30 to 45°C (15°C d<sup>-1</sup>), however, losing all nitrifying activity. Slightly higher nitrification  
91 temperatures (42.5°C) were reached by Courtens et al. (2014a) who imposed smaller  
92 temperature differences (2.5°C d<sup>-1</sup>) from 40°C on. It was furthermore demonstrated that salt  
93 amendment can be used as a tool to reach more efficient temperature transitions. However,  
94 from those studies it is clear that no ‘real’ thermophilic (>45°C) nitrification can be achieved  
95 through a stepwise temperature increase pattern (> 2.5°C d<sup>-1</sup>), although short-term activity

96 measurements of mesophilic sludge (34°C) showed nitrifying potential up to 50°C (Lopez-  
97 Vazquez et al. 2014).

98 Therefore, in this study, the adaptive capacities of mesophilic nitrifying sludge to gradual  
99 temperature increase patterns were explored. In a first reactor experiment, a non-oscillating  
100 linear temperature increase ( $0.25^{\circ}\text{C d}^{-1}$ ) was compared with an oscillating increase (amplitude  
101  $2^{\circ}\text{C}$ ) with the same final slope. Pre-exposure to a certain stress can in some cases result in an  
102 increased resilience towards this stress as shown for copper stress in denitrifiers (Li et al.  
103 2014, Philippot et al. 2008). In a second experiment, a linear temperature increase with a  
104 lower slope ( $0.08^{\circ}\text{C d}^{-1}$ ) was investigated, in which a floccular growth system (SBR) was  
105 compared with a biofilm based system (MBBR). Biomass retention of the slow growing  
106 thermophilic autotrophs is essential, and could eventually be favored through a biofilm based  
107 reactor system. Finally, the nitrifying community was closely monitored by batch activity  
108 tests and molecular analyses during the linear temperature increase to elucidate the adaptation  
109 process or shifts in the microbial community.

## 110 2. Materials and methods

### 111 2.1. Reactor set-up and operation

112 An overview of the two reactor experiments and associated reactor parameters is presented in  
113 **Table 1**. In the first experiment with two identical lab-scale sequential batch reactors (SBR), a  
114 linear temperature increase ( $0.25^{\circ}\text{C d}^{-1}$ ) with (SBR<sub>1</sub>) and without (SBR<sub>2</sub>) an oscillation  
115 (amplitude  $2^{\circ}\text{C}$ , frequency  $0.088 \text{ d}^{-1}$ ) were compared. In the second reactor experiment, a  
116 lower linear temperature increase ( $0.08^{\circ}\text{C d}^{-1}$ ) was applied, and a SBR (SBR<sub>3</sub>) was compared  
117 with a MBBR. The majority of the process and feeding parameters were the same in all  
118 reactors to investigate the effect of temperature pattern and/or sludge aggregation (flocs  
119 versus biofilm) (**Table 1**).

120 The reactor vessels (working volume 2 L, diameter 12 cm) were jacketed, allowing  
121 temperature control with a circulating thermostatic water bath, and equipped with a stirring  
122 device. The reactor pH was controlled between pH 6.5 and 7.5 by dosage of 0.1 M  
123 NaOH/HCl, and continuous aeration was provided by air pumps through a diffuser stone. The  
124 synthetic medium consisted of  $(\text{NH}_4)_2\text{SO}_4$  ( $10\text{-}800 \text{ mg N L}^{-1}$ ),  $11\text{-}12 \text{ g NaHCO}_3 \text{ g}^{-1} \text{ N}$ ,  
125  $\text{KH}_2\text{PO}_4$  ( $10 \text{ mg P L}^{-1}$ ) and  $0.1 \text{ mL L}^{-1}$  trace element solution dissolved in tap water (Kuai and  
126 Verstraete 1998). The nitrogen loading was adjusted through the ammonium concentration in  
127 the influent. The 6- and 4-h cycle of the SBR consisted of a 330 and 210-min aerobic reaction  
128 period including three 25-min feeding periods, a 15-min settling period, a 5-min decanting  
129 period and a 10-min idle period.

130 The carrier material of the MBBR consisted of polyvinyl alcohol (PVA)-gel beads (Kuraray,  
131 Japan) at a volumetric filling ratio of 15%. All reactors were inoculated with the same  
132 commercial nitrifying inoculum (Avecom NV, Ghent, Belgium) at an initial biomass  
133 concentration of  $2.4 \pm 0.1 \text{ g volatile suspended solids (VSS) L}^{-1}$ . To ensure sufficient biomass

134 growth on the carriers of the MBBR, a stabilization period (79 days) was included in the  
135 second experiment. The MBBR was initially operated in the same sequencing batch  
136 feeding/withdrawal mode during the stabilization period to ensure enough suspended biomass  
137 for biomass growth on the carriers. Once growth was observed on the carriers, initially, half  
138 of the suspended biomass was wasted (day 23 of the stabilization period). Further on, the  
139 residual suspended biomass was gradually wasted at about 45 mg VSS d<sup>-1</sup> until day 79 when  
140 the settling period was excluded.

## 141 **2.2. Ex-situ nitrification activity tests**

142 In parallel with the second reactor experiment, batch activity tests were performed with the  
143 SBR<sub>3</sub> sludge and MBBR carriers to monitor the progress of the optimal temperature for both  
144 ammonia and nitrite oxidation. Temperature sensitivity measurements were performed at  
145 reactor temperatures of 38°C, 40°C, 42°C, 44°C, 46°C and 48°C, in which the specific  
146 ammonia and nitrite oxidizing activities were measured at the respective reactor temperature  
147 ±2°C. For the SBR<sub>3</sub> sludge, 96-well plates with a working volume of 250 µL were used, while  
148 the MBBR carriers were transferred in 24-well plates with a working volume of 1.5-2.5 mL.  
149 Plates were incubated in a MB100-4A Thermoshaker (Hangzhou Allsheng Instruments,  
150 China) at the specific temperature, in which oxygen was provided through intensive shaking  
151 at 600 rpm. The buffer solution (pH 7) contained final concentrations of 2 g P L<sup>-1</sup>  
152 (KH<sub>2</sub>PO<sub>4</sub>/K<sub>2</sub>HPO<sub>4</sub>), 1 g NaHCO<sub>3</sub> L<sup>-1</sup> and 60 mg N L<sup>-1</sup> ((NH<sub>4</sub>)<sub>2</sub>SO<sub>4</sub> or NaNO<sub>2</sub>). The sensitivity  
153 of ammonia and nitrite oxidation for free ammonia (FA) was also evaluated by determining  
154 the specific activity at different ammonium concentrations (25-200 mg N L<sup>-1</sup>). All treatments  
155 were performed in sextuple, and liquid samples (2 µL) were taken over time for NH<sub>4</sub><sup>+</sup> and  
156 NO<sub>2</sub><sup>-</sup> analysis. These high-throughput activity measurements were highly optimized for each  
157 sludge type prior to the actual tests, demonstrating no oxygen limitation as increased shaking  
158 speed (250-600 rpm) did not increase nitrogen oxidation rates. A validation experiment was



159 performed in which the obtained rates were not significantly different with rates obtained in  
160 conventional 250 mL Erlenmeyer aerobic batch tests without oxygen limitation as monitored  
161 with an online DO measurement (Windey et al. 2005).

### 162 **2.3. Sludge production and settleability**

163 Sludge production was evaluated through the observed sludge yield (Y), calculated using  
164 cumulative terms, as described previously (Courtens et al. 2014b). Biomass settleability of the  
165 floccular sludge was measured through the determination of the sludge volume index (SVI) in  
166 a 1 L Imhoff cone, with the sludge height variation monitored for 5 min instead of 30 min to  
167 prevent extensive cooling of the sludge.

### 168 **2.4. Molecular analyses**

169 Biomass samples ( $\pm 2$  g) of the inoculum and the reactors (SBR<sub>3</sub> and MBBR) were collected  
170 over time, and total DNA was extracted using the Fast-Prep24 instrument (MP-BIO,  
171 Germany) as described previously (Vilchez-Vargas et al. 2013). DNA quality and quantity  
172 were analysed electrophoretically on 1% (w/v) agarose gel and spectrophotometrically by  
173 determination of the absorbance ratios at 260 nm and 280 nm and the absorbance at 260nm,  
174 using a NanoDrop ND-1000 instrument (Thermo Scientific), respectively. Abundance of the  
175 16S ribosomal RNA (rRNA) genes of *Nitrospira* spp. and *Nitrobacter* spp. and the functional  
176 gene encoding the A subunit of the bacterial and archaeal monooxygenase (*amoA*) was  
177 monitored using quantitative PCR (qPCR) assays on an ABI StepOnePlus real-time PCR  
178 instrument (Life Technologies, Carlsbad, CA, USA). Whereas *amoA* abundance is a good  
179 proxy for monitoring AOB and AOA abundance, the genera *Nitrospira* and *Nitrobacter*  
180 represent major NOB. Reactions were performed in a total volume of 20  $\mu$ l consisting of 10  $\mu$ l  
181 of iTaq Universal SYBR Green Supermix (Bio-Rad Laboratories, Hercules, CA, USA), 1.0  $\mu$ l  
182 DNA template (diluted), 0.3 (*Nitrobacter*), 0.5 (*amoA*) or 0.6  $\mu$ l (*Nitrospira*) of each forward

183 and reverse primer, adjusted to a final volume of 20  $\mu\text{l}$  with  $\text{H}_2\text{O}$  (Table S1). Amplifications  
184 were run as follows: initial denaturation for 2 min at 95 °C followed by 40 cycles of 15 s  
185 denaturation at 94 °C, 30 s annealing at the temperature mentioned in Table S1 (supplemental  
186 information) and 30 s elongation at 60 °C. Each sample extract was amplified in triplicate and  
187 target quantification was performed using a standard curve. Standard curves (range: 1.0E+02 -  
188 1.0E+07 copies  $\mu\text{l}^{-1}$ ) were generated using six ten-fold dilutions of target DNA from  
189 Fosmid54D9 (Treusch et al. 2005), *Nitrosomonas europaea* DSM 28437, *Nitrobacter*  
190 *winogradskyi* DSM 10237 and *Nitrospira moscoviensis* DSM 10035. Additional  
191 positive/negative controls and a melting curve analysis were performed in all analyses to  
192 verify target specific amplification, the absence of contaminants, and to confirm product  
193 specificity, respectively.

194 The overall community structure was analyzed using paired-end high-throughput sequencing  
195 (MiSeq Illumina platform) of amplified V5-V6 regions of the 16S rRNA gene, using the  
196 universal primers 807F and 1050R (Bohorquez et al. 2012). Amplification, library  
197 preparations, sequencing and bioinformatic processing of sequences was done according to  
198 Camarinha-Silva et al. (2014) with some modifications. Prior to the addition of barcodes and  
199 Illumina adapters the template was enriched by 20 PCR cycles using primers 807F and  
200 1050R. Raw sequences were assembled (Cole et al. 2014) and subsequently aligned using  
201 MOTHUR (gotoh algorithm with the SILVA reference database) prior to preclustering  
202 allowing two mismatches (Schloss et al. 2009). Next, sequences were clustered at a sequence  
203 similarity cut-off value of 99% to define species-level operational taxonomic units (OTUs).  
204 Only OTUs (phylotypes,Phy) exhibiting an average abundance of at least 0.001% of the total  
205 communities and a sequence length >200bp were considered for further analysis.  
206 Phylogenetic analyses were performed with MEGA5 (Tamura et al. 2011) using the neighbor-  
207 joining method with Jukes-Cantor correction and pairwise deletion of gaps/missing data. A

208 total of 1000 bootstrap replications were performed to test for branch robustness. A heat map  
209 was generated using gplots and RColorBrewer packages.

210

## 211 **2.5. Chemical analyses**

212 Ammonium (Nessler method), total suspended solids (TSS) and volatile suspended solids  
213 (VSS) were measured according to standard methods (Greenberg et al. 1992). The biomass  
214 concentration in the MBBR was determined through extraction of the biomass from the PVA  
215 carriers and subsequent protein measurement. The protein content was then translated to a  
216 VSS concentration using the average protein content of the MBBR sludge,  $0.31 \text{ g protein g}^{-1}$   
217  $\text{VSS}_{\text{MBBR sludge}}$  as determined. The carriers were cut in fine pieces and incubated in 1 M NaOH  
218 for 2 hours at  $46^{\circ}\text{C}$  with regular mixing for biomass extraction. To determine the protein  
219 concentration in the extract, the method developed by Lowry was used with bovine serum  
220 albumin (BSA) as the standard (Lowry et al. 1951). Nitrite and nitrate were determined on a  
221 930 Compact Ion Chromatograph (Metrohm, Switzerland), equipped with a conductivity  
222 detector. Dissolved oxygen (DO) and pH were measured with an HQ30d DO meter (Hach  
223 Lange, Germany) and a Dulcotest pH-electrode PHEP 112 SE (Prominent, Germany),  
224 respectively. In the batch activity tests, the liquid samples for ammonium and nitrite  
225 determination were always immediately analyzed spectrophotometrically with the Berthelot  
226 and Montgomery reaction, including a triplicate standard curve for each analysis run.  
227 Measurements were obtained using a Tecan infinite plate reader (Tecan, Switzerland), and  
228 biomass was quantified through protein concentrations.

229

## 230 **3. Results**

### 231 **3.1. Oscillating versus non-oscillating linear temperature increase**

232 The adaptive capacities of mesophilic nitrifying sludge were first evaluated for two different  
233 gradual temperature increase patterns. An oscillating temperature increase with an amplitude  
234 of 2°C and a frequency of 0.088 d<sup>-1</sup> was compared with a non-oscillating increase with the  
235 same linear slope (0.25°C d<sup>-1</sup>) as shown in **Figure 1**. Prior to any temperature increase, the  
236 reactors were started up identically at 37°C reaching ammonium removal rates of 180 ± 14  
237 mg N L<sup>-1</sup> d<sup>-1</sup> or 136 ± 10 mg N g VSS<sup>-1</sup> d<sup>-1</sup> after one week of stabilization. Nitrite  
238 accumulation was negligible in both reactors and nitrate production accounted for 95% of the  
239 ammonium removal. Up to 40°C, no changes in volumetric ammonium removal rates were  
240 observed in both reactors. Further temperature increase above 40°C, however, negatively  
241 affected the nitrifying activity in both reactors, with a more pronounced effect in the  
242 oscillating reactor. At 42°C, only 15% of the initial volumetric nitrifying activity remained in  
243 the oscillating reactor (26 ± 5 mg N L<sup>-1</sup> d<sup>-1</sup>) while 50% remained in the non-oscillating one  
244 (90 ± 3 mg N L<sup>-1</sup> d<sup>-1</sup>) (**Figure 1**). Although the non-oscillating reactor seemed to better resist  
245 the temperature increase, the decreasing trend pursued in both reactors finally resulting in an  
246 entire loss of activity at 45°C in both reactors, suggesting that the imposed slope of 0.25°C d<sup>-1</sup>  
247 was too high.

### 248 **3.2. Floccular versus biofilm based reactor system**

#### 249 **3.2.1. Reactor performance**

250 In the second reactor experiment, a linear temperature increase with a lower slope was  
251 investigated (0.08-0.16°C d<sup>-1</sup>), in which a SBR (SBR<sub>3</sub>) was compared with a MBBR (**Table**  
252 **1**). A 79-day stabilization period at 38°C allowed sufficient acclimatization of the inoculum  
253 and, more specifically, biomass growth on the PVA gel carriers of the MBBR. The suspended

254 biomass in the MBBR was gradually wasted during this period, while clear attached growth  
255 was observed on the PVA carriers (**Figure S1**). At the start of the actual experiment the  
256 settling was excluded to waste all the suspended sludge. This resulted in roughly a doubling  
257 of the attached growth (**Figure 2C**) and a further increase of the ammonium removal rate up  
258 to  $580 \pm 44 \text{ mg N L}^{-1} \text{ d}^{-1}$  (**Figure 2B**). As the SBR<sub>3</sub> sludge content also sharply increased  
259 from about  $3.3 \text{ g VSS L}^{-1}$  (day 6) to  $4.5 \text{ g VSS L}^{-1}$  (day 16), eventually endangering settling  
260 behavior, about one third of the SBR<sub>3</sub> sludge was wasted before the start of the temperature  
261 increase. Concurrently, the loading was lowered by one third to prevent overloading, reaching  
262 comparable volumetric nitrification rates in both reactors (**Figure 2B**). From day 20 on,  
263 temperature was gradually increased in both reactors at a slope of  $0.16^\circ\text{C d}^{-1}$  (**Figure 2A**). In  
264 accordance with the first reactor experiment, from  $38^\circ\text{C}$  to  $40^\circ\text{C}$ , no negative effect on the  
265 nitrification performance was observed. On the contrary, volumetric rates slightly increased  
266 (**Figure 2B**). As temperatures above  $40^\circ\text{C}$  initiated reactor failing in the first experiment  
267 (**Figure 1**), from  $40^\circ\text{C}$  on, the imposed slope was halved to  $0.08^\circ\text{C d}^{-1}$  (day 32). At that  
268 moment, a technical failure of the pH controller led to acidification (pH 5) in the MBBR  
269 resulting in a 18% decrease of nitrification performance. The MBBR recovered, even though  
270 temperature further increased. Stable ammonium removal rates of  $563 \pm 52 \text{ mg N L}^{-1} \text{ d}^{-1}$   
271 (SBR<sub>3</sub>) and  $358 \pm 40 \text{ mg N L}^{-1} \text{ d}^{-1}$  (MBBR) were observed in both reactors until  $45^\circ\text{C}$ . From  
272  $45.5^\circ\text{C}$  on, however, ammonium removal rates gradually decreased in the MBBR from  $358 \pm$   
273  $40$  to  $23 \pm 8 \text{ mg N L}^{-1} \text{ d}^{-1}$  at  $46.5^\circ\text{C}$  (**Figure 2B**). As more than 90% of the activity was lost,  
274 temperature increase was ceased in the MBBR. In contrast, volumetric rates increased in the  
275 SBR<sub>3</sub> up to  $776 \pm 62 \text{ mg N L}^{-1} \text{ d}^{-1}$  at a temperature as high as  $49^\circ\text{C}$ , corresponding with a  
276 specific ammonium removal rate of  $155 \pm 24 \text{ mg N g VSS}^{-1} \text{ d}^{-1}$  (**Figure 2C**). Nitrite  
277 accumulation was observed from temperatures higher than  $49^\circ\text{C}$  up to  $200 \text{ mg N L}^{-1}$ . As batch  
278 activity tests with SBR<sub>3</sub> sludge showed that nitrite concentrations up to  $500 \text{ mg N L}^{-1}$  did not

279 have a significant effect on the ammonium oxidizing activity ( $p < 0.05$ , **Figure S2**), the loading  
280 rate was not adjusted. At 49.5°C, a malfunctioning of the pH controller pump now also  
281 acidified the SBR<sub>3</sub> (pH 3-4), resulting in a decrease of ammonium removal activity to 30 mg  
282 N L<sup>-1</sup> d<sup>-1</sup>. The temperature in the SBR<sub>3</sub> was decreased to 48.5°C to allow for recovery of the  
283 SBR<sub>3</sub>. Ammonium oxidation rates increased again reaching >300 mg N L<sup>-1</sup> d<sup>-1</sup> after 50 days,  
284 while nitrite oxidation could not be recovered (**Figure S3**). Overall, the highest temperature  
285 where complete and stable nitrification was observed was 45.5°C and 49°C in the MBBR and  
286 SBR<sub>3</sub>, respectively.

### 287 **3.2.2. Community adaptation**

288 The adaptive capacity of the SBR<sub>3</sub> and MBBR sludge towards the imposed temperature  
289 increase was closely monitored with parallel batch activity tests. Every 2°C along the  
290 temperature increase, specific ammonium and nitrite oxidizing activities of both sludge types  
291 were measured at the respective reactor temperature and at plus and minus 2°C. The results of  
292 these batch activity tests are presented in **Figure 3**. Similar observations were made for both  
293 reactors up to 42°C. Although the differences were small, it appeared that between 38 and  
294 42°C, the temperature with the highest ammonium oxidizing activity was 40°C. Although the  
295 ammonium oxidation optimum in the SBR<sub>3</sub> gradually shifted from 40°C towards 46-48°C  
296 (**Figure 3A**), the MBBR optimum did not get higher than 42°C (**Figure 3B**). Moreover, at a  
297 reactor temperature of 44°C, no ammonium oxidation activity could be measured in the  
298 MBBR sludge at 46°C, clearly predicting the MBBR crash at 46°C (**Figure 3B**). Despite the  
299 loss of ammonium oxidation at 46°C, the batch activity test indicates that the MBBR's nitrite  
300 oxidizers were still active up to 48°C (**Figure 3D**). The nitrite oxidizers in the SBR<sub>3</sub> seemed  
301 to be adapted once the reactor reached 48°C, but a significant inhibition was observed at 50°C  
302 (**Figure 3C**). Indeed, temperatures higher than 49°C led to nitrite accumulation in the SBR<sub>3</sub>  
303 (**Figure 2B**).



### 305 **3.2.3. Free ammonia sensitivity**

306 Sensitivity of the nitrifying sludge towards elevated free ammonia (FA) was evaluated along  
307 the temperature increase. No significant inhibition of ammonium oxidation could be observed  
308 in both reactors by FA up to  $6 \text{ mg N L}^{-1}$ , in contrast, ammonium oxidation was stimulated by  
309 elevated FA (**Figure S4 A and B**).

310 The SBR<sub>3</sub>'s nitrite oxidizers were only slightly or not inhibited by FA up to  $6 \text{ mg N L}^{-1}$  at the  
311 lower operating temperatures (38-42°C), but were strongly inhibited at 46-48°C with a 50%  
312 (IC<sub>50</sub>) and 100% (IC<sub>100</sub>) inhibitory concentration of  $0.67 \pm 0.01$  and  $1.42 \pm 0.08 \text{ mg NH}_3\text{-N L}^{-1}$ ,  
313 respectively (**Figure S4 C**). The opposite trend was observed in the MBBR. Nitrite  
314 oxidation was clearly inhibited at 38-40°C, with an IC<sub>50</sub> of  $0.48 \pm 0.07 \text{ mg NH}_3\text{-N L}^{-1}$ , while  
315 the inhibition by FA disappeared at elevated temperatures (44-46°C) (**Figure S4 D**), possibly  
316 due to an increased diffusion limitation as the biomass concentration in the MBBR, and thus  
317 thickness of the biomass, strongly increased over time/temperature.

### 318 **3.2.4. Sludge production and settleability**

319 The increasing temperature initially induced a sharp decrease in sludge production in the  
320 SBR<sub>3</sub>. The observed sludge yield halved from  $0.074$  to  $0.035 \text{ g VSS g}^{-1} \text{ N}$  from 38°C to 42°C,  
321 whereas it increased again from 44°C to a yield of  $0.067 \pm 0.005 \text{ g VSS g}^{-1} \text{ N}$  up to 48°C  
322 (**Figure S5**). In contrast, sludge production in the MBBR was equal to  $0.11 \text{ g VSS g}^{-1} \text{ N}$  until  
323 42°C, whereupon it decreased and finally became negative at 46°C as a result of biomass die  
324 off (**Figure 2C**). Settling behavior of the SBR<sub>3</sub> sludge was stable up to 44°C, with a SVI<sub>5</sub> of  
325  $241 \pm 38 \text{ mL g}^{-1}$ , and improved at 46-48°C with a SVI<sub>5</sub> of  $154 \pm 2 \text{ mL g}^{-1}$  (**Figure S5**). The  
326 sludge residence time (SRT) in the SBR<sub>3</sub> was  $92 \pm 7$  days, while the SRT of the MBBR was  
327 considered infinite as nearly no suspended sludge could be measured in the effluent.

328



### 329 3.2.5. Functional community analysis

330 The abundance of selected key groups of nitrifying microorganisms was assessed along the  
331 temperature increase by means of qPCR. The reactors were inoculated with a subsample of  
332 the same inoculum, comprising a relatively well-balanced amount of AOB versus AOA  
333 ( $2.1 \times 10^9$  versus  $3.5 \times 10^8$  *amoA* gene copies  $\text{g}^{-1}$  VSS) and of the nitrite oxidizers *Nitrospira*  
334 spp. versus *Nitrobacter* spp. ( $6.7 \times 10^9$  versus  $4.8 \times 10^{10}$  16S gene copies  $\text{g}^{-1}$  VSS). The AOB  
335 dominance was preserved in both reactors after the stabilization period reaching an  
336 AOB/AOA ratio of 279 and 7091 in the SBR<sub>3</sub> and MBBR, respectively. The bacterial *amoA*  
337 gene abundance kept stable up to 45°C at around  $10^{10}$  copies  $\text{g}^{-1}$  VSS in both reactors, and  
338 then gradually decreased (**Figure 2D**). Clear differences in AOA abundances were, however,  
339 observed between the different reactors. The MBBR biomass retained significantly less AOA  
340 compared with the SBR<sub>3</sub> sludge after the stabilization period (**Figure 2D**, day 16). Moreover,  
341 a steep increase in AOA abundance by 3 orders of magnitude was observed in the SBR<sub>3</sub> at  
342 about 44°C, rising from  $1.0 \times 10^7$  to  $2.9 \times 10^{10}$  copies  $\text{g}^{-1}$  VSS, while the AOA abundance in the  
343 MBBR only slightly increased by two orders of magnitude to  $8.6 \times 10^8$  copies  $\text{g}^{-1}$  VSS at 46°C.  
344 This shows a clear shift in dominant ammonia oxidizers in the SBR<sub>3</sub> from AOB to AOA from  
345 45°C on, while this shift never completely occurred in the MBBR. For nitrite oxidation,  
346 *Nitrospira* spp. were dominant over *Nitrobacter* spp. in both reactors over the whole  
347 experiment (**Figure 2D**). The observed trends in key nitrifier abundances were confirmed by  
348 community structure analysis through sequencing of the V5V6 region of the 16S rRNA gene  
349 (**Figure S6**). The most dominant AOB retrieved in the MBBR (Phy1) appeared to belong to  
350 the *Nitrosomonas europaeae* species (**Figure S7**) and the most dominant AOA in the SBR<sub>3</sub>  
351 (Phy8) as well as the inoculum (Phy56) belonged to the *Nitrososphaera* genus (**Figure 4**).  
352 Interestingly, this AOA (Phy8) only showed a 95% similarity with the AOA initially detected

353 in the inoculum (Phy56). The closest related known NOB of the dominant *Nitrospira* in both  
354 reactors is *Nitrospira japonica J1* with 91% similarity (**Figure 5**).

355

## 356 4. Discussion

### 357 4.1. Overall performance

358 The adaptive capacities of mesophilic nitrifying sludge over different linear temperature  
359 increase patterns and different sludge growth modes were explored in this study of which the  
360 main results are summarized in **Table 1**. A non-oscillating temperature pattern (SBR<sub>2</sub>)  
361 appeared to be more effective than an oscillating pattern (SBR<sub>1</sub>) for the tested slope of 0.25°C  
362 d<sup>-1</sup> as both the volumetric as specific rates were 2-3 times higher. In general, the ‘low-slope’  
363 reactors (SBR<sub>3</sub> and MBBR) reached 3 to 30 times higher volumetric rates than the ‘high-  
364 slope’ reactors (SBR<sub>1</sub> and SBR<sub>2</sub>), at significantly higher temperatures. Finally, the biofilm  
365 based system (MBBR) showed 2.5 times lower rates than the parallel floccular growth system  
366 (SBR<sub>3</sub>). Overall, within the range of the tested parameters/combinations in this study, the  
367 highest temperature with moreover the highest volumetric and specific nitrification rates were  
368 achieved through the transition of mesophilic nitrifying sludge by a slow, non-oscillating  
369 linear temperature increase (SBR<sub>3</sub>).

370 The successful transition of the SBR<sub>3</sub> towards thermophilic temperatures was, remarkably,  
371 accompanied with a change in observed sludge production (**Figure S5**). The decreasing trend  
372 sharply reversed at 44°C finally resulting in comparable observed sludge yields at 38°C and  
373 48°C ( $0.0687 \pm 0.005$  g VSS g<sup>-1</sup> N). It is possible that the temperature window 38-42°C can  
374 be considered as sub-optimal for both mesophiles and thermophiles, leading to increased  
375 decay rates and/or decreased growth rates, and hence a significantly lower net biomass  
376 production. Overall, the observed sludge yields were lower than reported values for  
377 combined AOB and NOB sludge yield of 0.19-0.21 g VSS g<sup>-1</sup> N at mesophilic temperatures  
378 (Barnes and Bliss 1983, Henze et al. 2008). Although shifts in net biomass production, i.e. the  
379 observed yield, coincided with the AOA vs. AOB dominance shift in this study, future

380 research should map the underlying biokinetic parameters. Besides growth and decay rate,  
381 also the oxygen and nitrogen affinity constants of the respective nitrifiers at different  
382 temperatures deserve attention to allow accurate modeling of nitrification at any elevated  
383 temperature.

384 In parallel, a clear shift in optimum temperature was observed with the ex-situ activity  
385 measurements. These small, fast, high-throughput activity tests, based on simple  
386 spectrophotometrical measurements, could predict the loss of ammonium and nitrite oxidation  
387 in the MBBR and SBR<sub>3</sub> (**Figure 3**), respectively. One could thus lower the slope of the  
388 imposed temperature slope when the optimum does not seem to evolve with the current  
389 temperature and so, steer the temperature increase strategy to achieve thermophilic  
390 nitrification.

#### 391 **4.2. Temperature increase pattern**

392 Pre-exposure to a certain stress can result in an increased resilience to a secondary exposure  
393 (Philippot et al. 2008, Ryall et al. 2012). In the framework of this study, a pre-exposure to an  
394 elevated temperature can e.g. induce the production of heat-shock proteins (HSP) that could  
395 possibly protect the biomass during a secondary temperature increase and so, improve the  
396 adaptive capabilities. This study however showed that the tested oscillating temperature  
397 pattern did not improve the adaptive capabilities of mesophilic nitrifying sludge towards  
398 higher temperatures (**Figure 1**). The tested amplitude of 2°C was possibly too high to observe  
399 beneficial effects and thus, smaller oscillating could eventually give better results.

400 The linear character of the imposed temperature pattern in this study was clearly more  
401 successful than stepwise temperature increases reaching only maximum nitrification  
402 temperatures of 40 and 42.5°C (Courtens et al. 2014a, Shore et al. 2012). This is in line with  
403 observations at a lower temperature range (10-20°C) in which the negative effect of a sudden

404 temperature decrease on nitrification was much stronger than a gradual temperature decrease  
405 (Hwang and Oleszkiewicz 2007). Although nitrifiers are known to cope with relatively high  
406 seasonal temperature changes in wastewater treatment plants in moderate climates (e.g. 10°C-  
407 30°C at DC Water, Washington, USA), this study showed that a relatively low slope in  
408 temperature increase was essential to allow the transition of nitrifiers to temperatures higher  
409 than 38°C-42°C.

### 410 **4.3. Sludge growth mode**

411 A floccular growth system (SBR<sub>3</sub>) was compared with a biofilm based system (MBBR), as  
412 biomass retention of the slow growing autotrophs is essential during the transition process,  
413 and could eventually be favored through a biofilm based reactor system. Experiences with  
414 thermophilic carbon treatment showed that thermophilic aerobic processes suffer from poor  
415 sludge settling properties (Suvilampi and Rintala 2003), thus, operation of settling based  
416 system such as a SBR may be threatened. Remarkably, settling behavior of the SBR<sub>3</sub> sludge  
417 in this study did not deteriorate (**Figure S5**), resulting in only minor differences in sludge  
418 retention time between both reactors.

419 The MBBR was initially hypothesized to better cope with the temperature transition, as  
420 biofilms show increased resistance to many types of environmental challenges (Gilbert et al.  
421 2002). Recently, Gilbert et al. (2015) showed that nitrate production in a partial  
422 nitritation/anammox MBBR was more resilient against a gradual temperature reduction (20°C  
423 to 10°C, 0.07 °C d<sup>-1</sup>), compared with a SBR, though ammonium oxidation declined similarly  
424 in both reactor types. Several observations, such as the increased resistance of biofilms  
425 towards antibiotics, are mainly explained by the restricted diffusion (Mah and O'Toole 2001).  
426 Recently, other factors, such as slow growth rate, high culture density and heterogeneity, were  
427 shown to influence the general stress response in biofilms (Mah and O'Toole 2001, Ryall et

428 al. 2012), and could eventually favor the adaptive capacities of nitrifiers towards elevated  
429 temperatures. This study is however in contrast with this hypothesis, as the ammonium  
430 oxidation MBBR failed around 46°C, while it could still be maintained until 49°C in the  
431 SBR<sub>3</sub> (**Figure 2B**). The successful transition in the SBR<sub>3</sub> seemed to be related to the observed  
432 shift of AOB to AOA dominance that was not completely achieved in the MBBR (**Figure**  
433 **2D**). This is in accordance with literature, where most described thermophilic ammonium  
434 oxidizers are archaeal (de la Torre et al. 2008, Hatzepichler et al. 2008, Lebedeva et al.  
435 2013). The slower growth rate of the nitrifiers in the MBBR, initially supposed to favor the  
436 general stress response on a short term (Ryall et al. 2012), probably delayed the essential  
437 selection process on a long term. Indeed, an increase in AOA abundance in the biofilm was  
438 also observed, though one month later than in the SBR<sub>3</sub> (**Figure 2D**). Furthermore, although  
439 both reactors were inoculated with the same AOA/AOB ratio, the relative decrease in AOA  
440 during the stabilization period was more pronounced in the biofilm than in the flocs resulting  
441 in an initially lower AOA abundance in the biofilm. The late start of the increasing trend of  
442 AOA in the MBBR suggests that the essential shift could eventually also have been achieved  
443 with an even lower slope of temperature increase. Potentially a stronger selection for fast  
444 growing micro-organisms was made in the MBBR versus the SBR giving more advantage to  
445 the faster growing AOB. Another possible reason for the differential stimulation of AOA vs.  
446 AOB in both systems might be the levels and dynamics of DO and NH<sub>4</sub><sup>+</sup> concentrations, as  
447 key substrates for ammonia oxidation and potentially niche differentiation. Figure S8 displays  
448 the typical concentration profiles, highlighting more frequent fluctuations of the bulk  
449 concentrations of both substrates along with lower concentrations of NH<sub>4</sub><sup>+</sup> in the SBR  
450 compared to the MBBR, possibly favoring AOA stimulation. Future research should focus on  
451 the actual substrate availability for the ammonia oxidizers within the flocs versus biofilm.

452 Besides the actual abundance of AOA in the biofilm, different, less thermotolerant, AOA  
453 species could have been enriched in the biofilm, compared with the floccular sludge.

454 Observations regarding nitrite oxidation were in line with literature, stating that *Nitrospira* is  
455 the most dominant nitrite oxidizer up to 60°C (Edwards et al. 2013, Lebedeva et al. 2011,  
456 Marks et al. 2012). In this study, no shifts were observed, and *Nitrospira* was dominant in  
457 both reactors over the entire experiment (**Figure 2D**). However, remarkable differences in  
458 free ammonia sensitivity were observed between reactors and over time (**Figure S4**),  
459 suggesting that a possible selection on strain level occurred during the transition. Overall,  
460 nitrite oxidizers were much more sensitive compared with the ammonium oxidizers, finally  
461 resulting in the development of a partial nitrification reactor at 48.5°C, opening opportunities  
462 for short-cut nitrogen removal processes.

#### 463 **4.4. Practical implications**

464 The results of this study suggest that existing mesophilic nitrifying wastewater plants can be  
465 upgraded to thermophilic systems through a slow, non-oscillating linear temperature increase.  
466 Excluding the stabilization period, which is non-relevant for existing plants, this could be  
467 achieved in about 140 days. Close monitoring of the transition by high-throughput activity  
468 tests as described in this study, could moreover allow an even faster transition period. It  
469 should be emphasized that, beside the temperature increase pattern, the presence of AOA in  
470 the mesophilic sludge appeared to be essential for a successful transition. The fact that AOA  
471 appear to be distributed in wastewater treatment plants worldwide, even in equal or higher  
472 abundance than AOB (Limpiyakorn et al. 2013), opens thus opportunities for thermophilic  
473 nitrogen removal.

474

#### 475 **5. Conclusions**

- 476 • The oscillating temperature pattern with an amplitude of 2°C and a slope of 0.25°C d<sup>-1</sup>  
477 achieved a low nitrification rate of 26 ± 5 mg N L<sup>-1</sup> d<sup>-1</sup> at 42°C and lost all activity at  
478 45°C.
- 479 • The moving bed biofilm reactor subjected to a slope of 0.08-0.16°C d<sup>-1</sup> was able to  
480 oxidize ammonium up to 46°C, though, at a low volumetric rate of 32 ± 7 mg N L<sup>-1</sup> d<sup>-1</sup>  
481 .
- 482 • Nitrification rates of up to 800 mg N L<sup>-1</sup> d<sup>-1</sup> and 170 mg N g VSS<sup>-1</sup> d<sup>-1</sup> were achieved  
483 at 49°C through gradual adaptation (0.08 °C d<sup>-1</sup>) of mesophilic nitrifying sludge in  
484 suspension (SBR<sub>3</sub>).
- 485 • The successful transition from mesophilic to thermophilic ammonia oxidation in SBR<sub>3</sub>  
486 was linked to a dominance shift of archaeal above bacterial ammonia oxidizers.
- 487 • Ex-situ batch activity measurements can serve as a good tool to monitor the process  
488 response to transition, predicting reactor failures, thus enabling steering of the  
489 temperature increase pattern.

490

## 491 **Acknowledgements**

492 E.N.P.C and S.E.V. were supported as doctoral candidate (Aspirant) and postdoctoral fellow,  
493 respectively, by the Research Foundation Flanders (FWO-Vlaanderen). R.V.V. was supported  
494 as a postdoctoral fellow from the Belgian Science Policy Office (BELSPO). The reactor  
495 equipment used for this study was by the King Baudouin Foundation. We thank José M.  
496 Carvajal-Arroyo for the assistance with the reactor experiment and Jo De Vrieze for the  
497 scientific discussions.



- 499 Barnes, D. and Bliss, P.J. (1983) Biological control of nitrogen in wastewater treatment, E. & F.N.  
500 Spon, London.
- 501 Bohorquez, L.C., Delgado-Serrano, L., Lopez, G., Osorio-Forero, C., Klepac-Ceraj, V., Kolter, R.,  
502 Junca, H., Baena, S. and Mercedes Zambrano, M. (2012) In-depth Characterization via  
503 Complementing Culture-Independent Approaches of the Microbial Community in an  
504 Acidic Hot Spring of the Colombian Andes. *Microbial Ecology* 63(1), 103-115.
- 505 Camargo, J.A. and Alonso, A. (2006) Ecological and toxicological effects of inorganic nitrogen  
506 pollution in aquatic ecosystems: A global assessment. *Environment International* 32(6),  
507 831-849.
- 508 Camarinha-Silva, A., Jáuregui, R., Chaves-Moreno, D., Oxley, A.P.A., Schaumburg, F., Becker, K.,  
509 Wos-Oxley, M.L. and Pieper, D.H. (2014) Comparing the anterior nare bacterial  
510 community of two discrete human populations using Illumina amplicon sequencing.  
511 *Environmental Microbiology* 16(9), 2939-2952.
- 512 Cole, J.R., Wang, Q., Fish, J.A., Chai, B., McGarrell, D.M., Sun, Y., Brown, C.T., Porras-Alfaro, A.,  
513 Kuske, C.R. and Tiedje, J.M. (2014) Ribosomal Database Project: data and tools for high  
514 throughput rRNA analysis. *Nucleic Acids Res* 42(Database issue), D633-642.
- 515 Courtens, E.N.P., Boon, N., De Schryver, P. and Vlaeminck, S.E. (2014a) Increased salinity  
516 improves the thermotolerance of mesophilic nitrification. *Applied Microbiology and*  
517 *Biotechnology* 98(10), 4691-4699.
- 518 Courtens, E.N.P., Vlaeminck, S.E., Vilchez-Vargas, R., Verliefde, A., Jauregui, R., Pieper, D.H. and  
519 Boon, N. (2014b) Trade-off between mesophilic and thermophilic denitrification: Rates  
520 vs. sludge production, settleability and stability. *Water Research* 63, 234-244.
- 521 de la Torre, J.R., Walker, C.B., Ingalls, A.E., Konneke, M. and Stahl, D.A. (2008) Cultivation of a  
522 thermophilic ammonia oxidizing archaeon synthesizing crenarchaeol. *Environmental*  
523 *Microbiology* 10(3), 810-818.
- 524 Edwards, T.A., Calica, N.A., Huang, D.A., Manoharan, N., Hou, W., Huang, L., Panosyan, H., Dong, H.  
525 and Hedlund, B.P. (2013) Cultivation and characterization of thermophilic *Nitrospira*  
526 species from geothermal springs in the US Great Basin, China, and Armenia. *FEMS*  
527 *Microbiol Ecol* 85(2), 283-292.
- 528 Erisman, J.W., Sutton, M.A., Galloway, J., Klimont, Z. and Winiwarter, W. (2008) How a century of  
529 ammonia synthesis changed the world. *Nature Geoscience* 1(10), 636-639.
- 530 Galloway, J.N., Winiwarter, W., Leip, A., Leach, A.M., Bleeker, A. and Erisman, J.W. (2014)  
531 Nitrogen footprints: past, present and future. *Environmental Research Letters* 9(11).
- 532 Gilbert, E.M., Agrawal, S., Schwartz, T., Horn, H. and Lackner, S. (2015) Comparing different  
533 reactor configurations for Partial Nitrification/Anammox at low temperatures. *Water*  
534 *Research* 81(0), 92-100.
- 535 Gilbert, P., Maira-Litran, T., McBain, A.J., Rickard, A.H. and Whyte, F.W. (2002) Advances in  
536 *Microbial Physiology*, pp. 203-256, Academic Press.
- 537 Greenberg, A.E., Clesceri, L.S. and Eaton, A.D. (1992) Standard Methods for the Examination of  
538 *Water and Wastewater*, American Public Health Association, Washington DC.
- 539 Hatzenpichler, R., Lebedeva, E.V., Spieck, E., Stoecker, K., Richter, A., Daims, H. and Wagner, M.  
540 (2008) A moderately thermophilic ammonia-oxidizing crenarchaeote from a hot spring.  
541 *Proceedings of the National Academy of Sciences of the United States of America* 105(6),  
542 2134-2139.
- 543 Henze, M., Van Loosdrecht, M., Ekama, G. and Brdjanovic, D. (2008) *Biological Wastewater*  
544 *Treatment: Principles, Modelling and Design*, IWA Publishing, London.
- 545 Hwang, J.H. and Oleszkiewicz, J.A. (2007) Effect of cold-temperature shock on nitrification. *Water*  
546 *Environ Res* 79(9), 964-968.
- 547 Kuai, L.P. and Verstraete, W. (1998) Ammonium removal by the oxygen-limited autotrophic  
548 nitrification-denitrification system. *Applied and Environmental Microbiology* 64(11),  
549 4500-4506.

550 Lackner, S., Gilbert, E.M., Vlaeminck, S.E., Joss, A., Horn, H. and van Loosdrecht, M.C.M. (2014)  
551 Full-scale partial nitrification/anammox experiences - An application survey. *Water*  
552 *Research* 55, 292-303.

553 Lapara, T.M. and Alleman, J.E. (1999) Thermophilic aerobic biological wastewater treatment.  
554 *Water Research* 33(4), 895-908.

555 Lebedeva, E.V., Hatzenpichler, R., Pelletier, E., Schuster, N., Hauzmayer, S., Bulaev, A., Grigor'eva,  
556 N.V., Galushko, A., Schmid, M., Palatinszky, M., Le Paslier, D., Daims, H. and Wagner, M.  
557 (2013) Enrichment and Genome Sequence of the Group I. 1a Ammonia-Oxidizing  
558 Archaeon "Ca. Nitrosotenuis uzonensis" Representing a Clade Globally Distributed in  
559 Thermal Habitats. *Plos One* 8(11).

560 Lebedeva, E.V., Off, S., Zumbraegel, S., Kruse, M., Shagzhina, A., Luecker, S., Maixner, F., Lipski, A.,  
561 Daims, H. and Spieck, E. (2011) Isolation and characterization of a moderately  
562 thermophilic nitrite-oxidizing bacterium from a geothermal spring. *Fems Microbiology*  
563 *Ecology* 75(2), 195-204.

564 Li, J., Zheng, Y.-M., Liu, Y.-R., Ma, Y.-B., Hu, H.-W. and He, J.Z. (2014) Initial Copper Stress  
565 Strengthens the Resistance of Soil Microorganisms to a Subsequent Copper Stress.  
566 *Microbial Ecology* 67(4), 931-941.

567 Limpiyakorn, T., Fuerhacker, M., Haberl, R., Chodanon, T., Srithep, P. and Sonthiphand, P. (2013)  
568 amoA-encoding archaea in wastewater treatment plants: a review. *Applied Microbiology*  
569 *and Biotechnology* 97(4), 1425-1439.

570 Lopez-Vazquez, C.M., Kubare, M., Saroj, D.P., Chikamba, C., Schwarz, J., Daims, H. and Brdjanovic,  
571 D. (2014) Thermophilic biological nitrogen removal in industrial wastewater treatment.  
572 *Applied Microbiology and Biotechnology* 98(2), 945-956.

573 Lowry, O.H., Rosebrough, N.J., Farr, A.L. and Randall, R.J. (1951) Protein measurement with the  
574 Folin phenol reagent. *J Biol Chem* 193(1), 265-275.

575 Mah, T.F. and O'Toole, G.A. (2001) Mechanisms of biofilm resistance to antimicrobial agents.  
576 *Trends in Microbiol* 9(1), 34-39.

577 Marks, C.R., Stevenson, B.S., Rudd, S. and Lawson, P.A. (2012) Nitrospira-dominated biofilm  
578 within a thermal artesian spring: a case for nitrification-driven primary production in a  
579 geothermal setting. *Geobiology* 10(5), 457-466.

580 Philippot, L., Cregut, M., Cheneby, D., Bressan, M., Dequiet, S., Martin-Laurent, F., Ranjard, L. and  
581 Lemanceau, P. (2008) Effect of primary mild stresses on resilience and resistance of the  
582 nitrate reducer community to a subsequent severe stress. *Fems Microbiology Letters*  
583 285(1), 51-57.

584 Ryall, B., Eydallin, G. and Ferenci, T. (2012) Culture history and population heterogeneity as  
585 determinants of bacterial adaptation: the adaptomics of a single environmental  
586 transition. *Microbiol Mol Biol Rev* 76(3), 597-625.

587 Schloss, P.D., Westcott, S.L., Ryabin, T., Hall, J.R., Hartmann, M., Hollister, E.B., Lesniewski, R.A.,  
588 Oakley, B.B., Parks, D.H., Robinson, C.J., Sahl, J.W., Stres, B., Thallinger, G.G., Van Horn, D.J.  
589 and Weber, C.F. (2009) Introducing mothur: open-source, platform-independent,  
590 community-supported software for describing and comparing microbial communities.  
591 *Appl Environ Microbiol* 75(23), 7537-7541.

592 Shore, J.L., M'Coy, W.S., Gunsch, C.K. and Deshusses, M.A. (2012) Application of a moving bed  
593 biofilm reactor for tertiary ammonia treatment in high temperature industrial  
594 wastewater. *Bioresource Technology* 112, 51-60.

595 Suvilampi, J. and Rintala, J. (2003) Thermophilic aerobic wastewater treatment, process  
596 performance, biomass characteristics, and effluent quality. *Reviews in Environmental*  
597 *Science and Biotechnology* 2(1), 35-51.

598 Tamura, K., Peterson, D., Peterson, N., Stecher, G., Nei, M. and Kumar, S. (2011) MEGA5:  
599 Molecular Evolutionary Genetics Analysis Using Maximum Likelihood, Evolutionary  
600 Distance, and Maximum Parsimony Methods. *Molecular Biology and Evolution* 28(10),  
601 2731-2739.

- 602 Treusch, A.H., Leininger, S., Kletzin, A., Schuster, S.C., Klenk, H.P. and Schleper, C. (2005) Novel  
603 genes for nitrite reductase and Amo-related proteins indicate a role of uncultivated  
604 mesophilic crenarchaeota in nitrogen cycling. *Environ Microbiol* 7(12), 1985-1995.
- 605 Vilchez-Vargas, R., Geffers, R., Suarez-Diez, M., Conte, I., Waliczek, A., Kaser, V.S., Kralova, M.,  
606 Junca, H. and Pieper, D.H. (2013) Analysis of the microbial gene landscape and  
607 transcriptome for aromatic pollutants and alkane degradation using a novel internally  
608 calibrated microarray system. *Environmental Microbiology* 15(4), 1016-1039.
- 609 Vlaeminck, S.E., De Clippeleir, H. and Verstraete, W. (2012) Microbial resource management of  
610 one-stage partial nitritation/anammox. *Microbial Biotechnology* 5(3), 433-448.
- 611 Windey, K., De Bo, I. and Verstraete, W. (2005) Oxygen-limited autotrophic nitrification-  
612 denitrification (OLAND) in a rotating biological contactor treating high-salinity  
613 wastewater. *Water Research* 39(18), 4512-4520.

614

615 **Table and Figure captions**

616 **Table 1.** Overview of reactor parameters, temperature increase patterns, volumetric and  
617 biomass specific rates achieved at the highest temperature where complete nitrification was  
618 observed in the two different reactor experiments. Averages calculated over at least 3  
619 hydraulic retention times ( $\pm 3$  operation days). n.a.: not applicable, SBR: sequencing batch  
620 reactor, MBBR: moving bed biofilm reactor, VER: volumetric exchange ratio, HRT:  
621 hydraulic retention time.

622

623 **Figure 1.** Temperature increase pattern **(A)** and nitrifying reactor performance **(B)** of two  
624 sequential batch reactors comparing a linear with an oscillating temperature increase ( $0.25^{\circ}\text{C}$   
625  $\text{d}^{-1}$ ).

626 **Figure 2.** Operation and performance characteristics of SBR<sub>3</sub> (left) and MBBR (right). **(A)**  
627 Temperature increase patterns. **(B)** Volumetric ammonium removal and nitrite/nitrate  
628 production rates. **(C)** Specific rates (left axis) and sludge content (right axis). **(D)** Abundance  
629 of nitrifiers as determined by qPCR.

630 **Figure 3.** Relative temperature activity curves for ammonium **(A,B)** and nitrite **(C,D)**  
631 oxidation of the SBR<sub>3</sub> **(A,C)** and MBBR **(B,D)** sludge. Each color curve represents a batch  
632 test performed at a certain reactor temperature, of which the temperature is indicated with a  
633 symbol. Per batch test, the temperature where the highest activity was measured was indicated  
634 as the 'optimum temperature' and assigned as 100%. All experiments were performed in  
635 sextuple, and statistically significant optima (student's t-test,  $p < 0.05$ ) are indicated with an  
636 asterisk.

637 **Figure 4.** Phylogenetic relationships between the most dominant archaeal 16S rRNA gene  
638 sequences in the SBR<sub>3</sub> reactor (Phy8) and the inoculum used (Phy56) and all described AOA

639 cultures or isolates, as well as relevant environmental clone sequences. Phy7 refers to the  
640 archaeal 16S rRNA gene sequence detected in the thermophilic nitrifying reactor enriched  
641 from compost by Courtens et al. (*Under review*).

642 **Figure 5.** Phylogenetic relationships between the most dominant *Nitrospira* 16S rRNA gene  
643 sequence in the SBR<sub>3</sub> and MBBR (Phy3) and all described *Nitrospira* cultures or isolates, as  
644 well as relevant environmental clone sequences. Phy1 refers to the *Nitrospira* 16S rRNA gene  
645 sequence detected in the thermophilic nitrifying reactor enriched from compost by Courtens et  
646 al. (*Under review*).

**Table 1**[Click here to download Table: Table 1.docx](#)

**Table 1.** Overview of reactor parameters, temperature increase patterns, volumetric and biomass specific rates achieved at the highest temperature where complete nitrification was observed in the two different reactor experiments. Averages calculated over at least 3 hydraulic retention times ( $\pm 3$  operation days). n.a.: not applicable, SBR: sequencing batch reactor, MBBR: moving bed biofilm reactor, VER: volumetric exchange ratio, HRT: hydraulic retention time.

Reactor(type)	Experiment 1		Experiment 2	
	SBR <sub>1</sub>	SBR <sub>2</sub>	SBR <sub>3</sub>	MBBR
<b>Linear temperature increase</b>	Oscillating	Steady	Steady	
<b>Linear slope (<math>^{\circ}\text{C d}^{-1}</math>)</b>	0.25		<40 $^{\circ}\text{C}$ : 0.16 >40 $^{\circ}\text{C}$ : 0.08	
<b>Oscillating amplitude (<math>^{\circ}\text{C}</math>)</b>	2	n.a.	n.a.	
<b>Oscillating frequency (<math>\text{d}^{-1}</math>)</b>	0.088	n.a.	n.a.	
<b>Experimental periods</b>				
Stabilization (d)	7		79	
Temperature increase (d)	50		150	
<b>VER (%)</b>	25		20	
<b>Cycle duration (h)</b>	6		4	
<b>Flowrate (L)</b>	$2.1 \pm 0.2$		$2.1 \pm 0.3$	
<b>HRT (d)</b>	$1.0 \pm 0.2$		$1.0 \pm 0.2$	
<b>Highest temperature (<math>^{\circ}\text{C}</math>)</b>	42	42	49	45.5
<b>Ammonium conversion rates*</b>				
Volumetric ( $\text{mg N L}^{-1} \text{d}^{-1}$ )	$26 \pm 5$	$90 \pm 3$	$794 \pm 57$	$309 \pm 30$
Specific ( $\text{mg N g}^{-1} \text{VSS d}^{-1}$ )	72**	$139 \pm 18$	$151 \pm 7$	67**

\* In all cases, nitrite accumulation was negligible and nitrate formation > 90% of ammonium removal

\*\* Only one biomass measurement available for the specific period

Figure 1  
[Click here to download high resolution image](#)

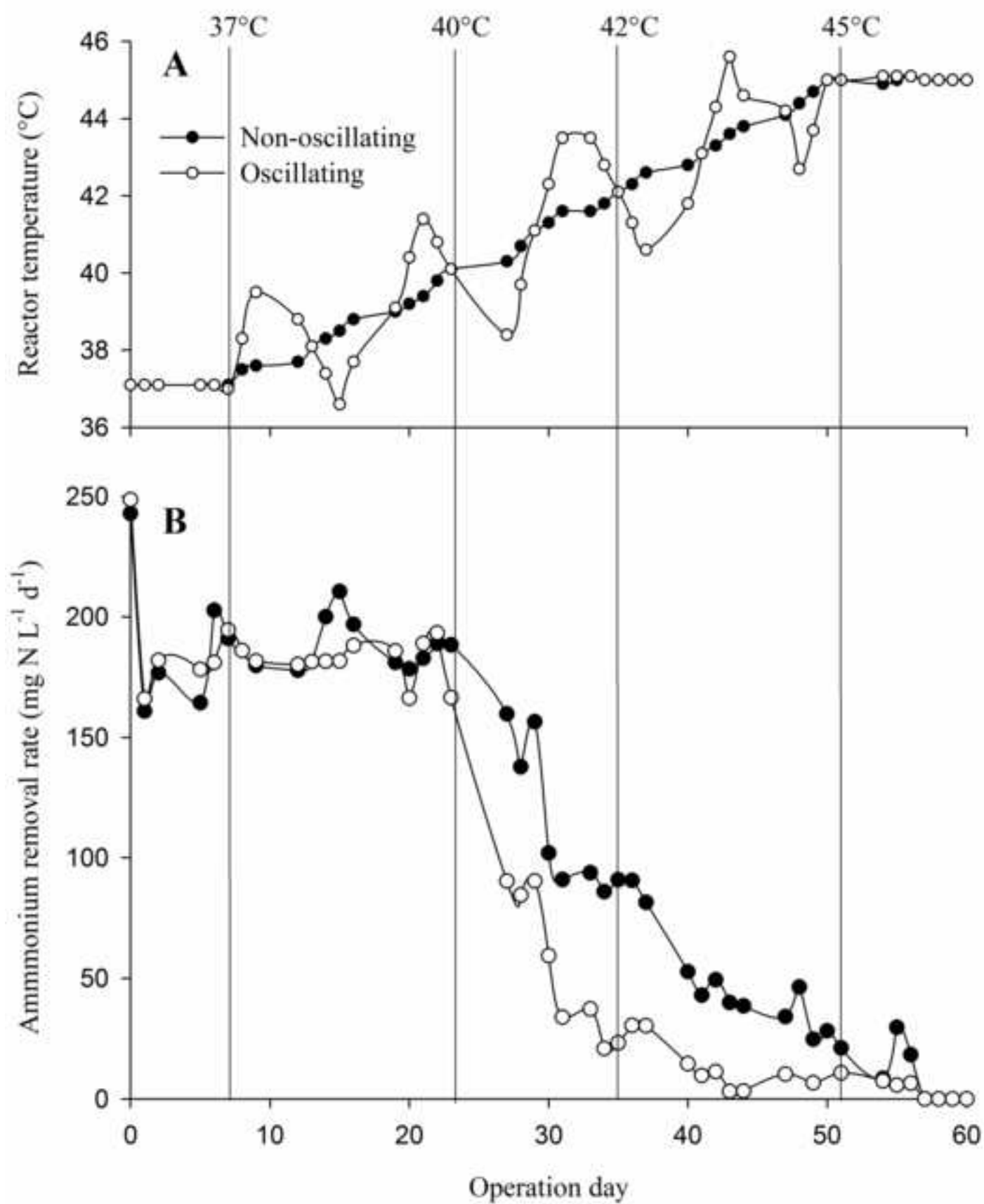


Figure 2

[Click here to download high resolution image](#)

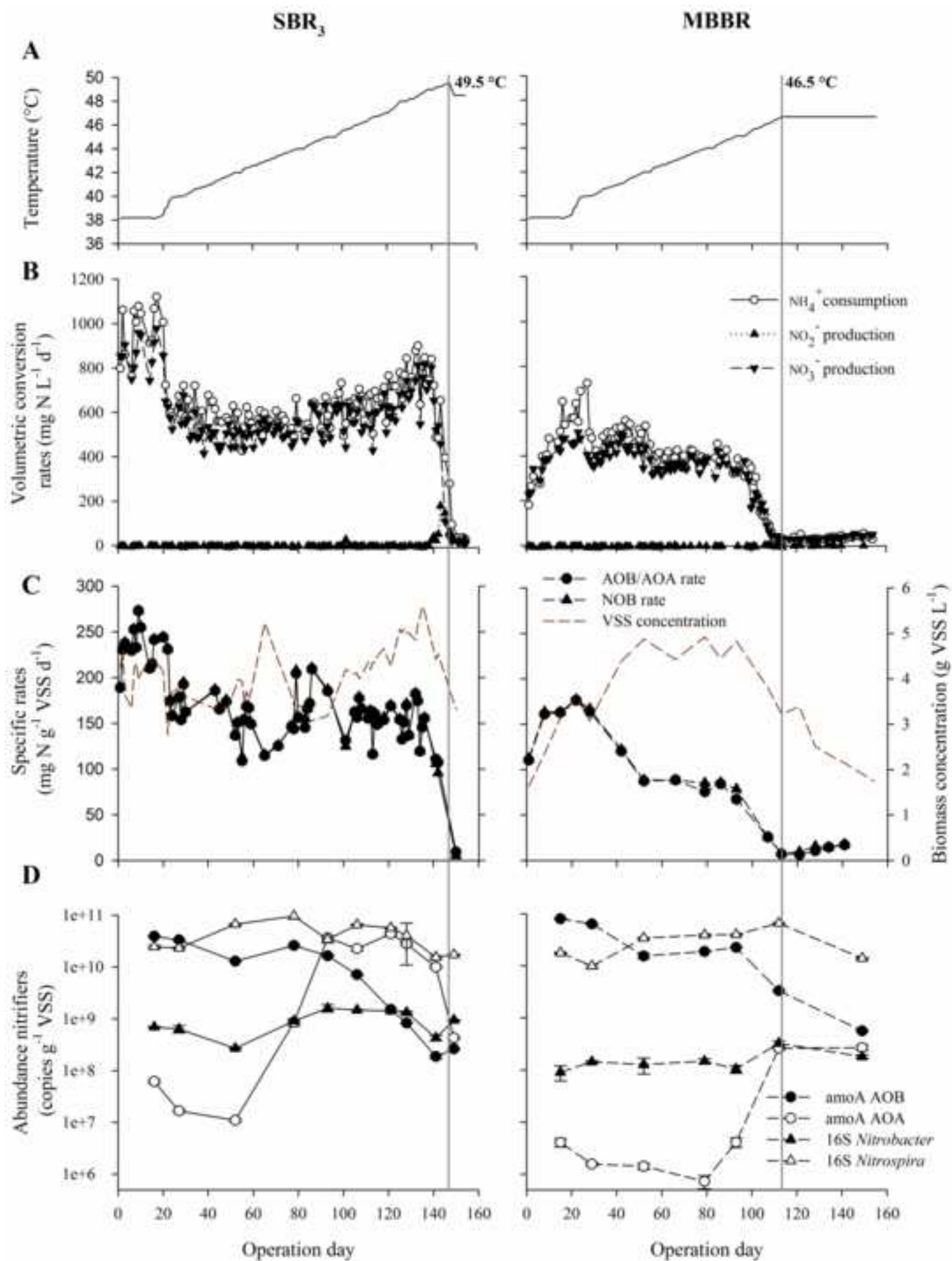




Figure 3  
[Click here to download high resolution image](#)

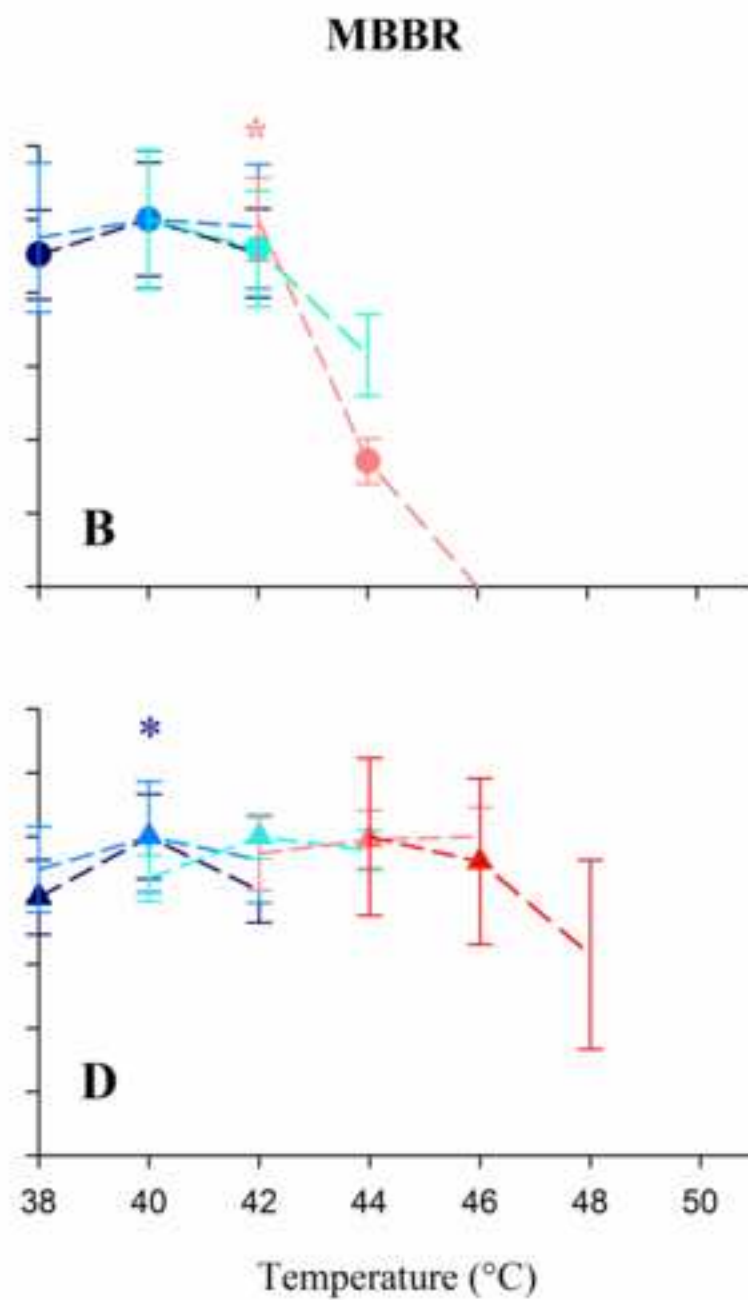
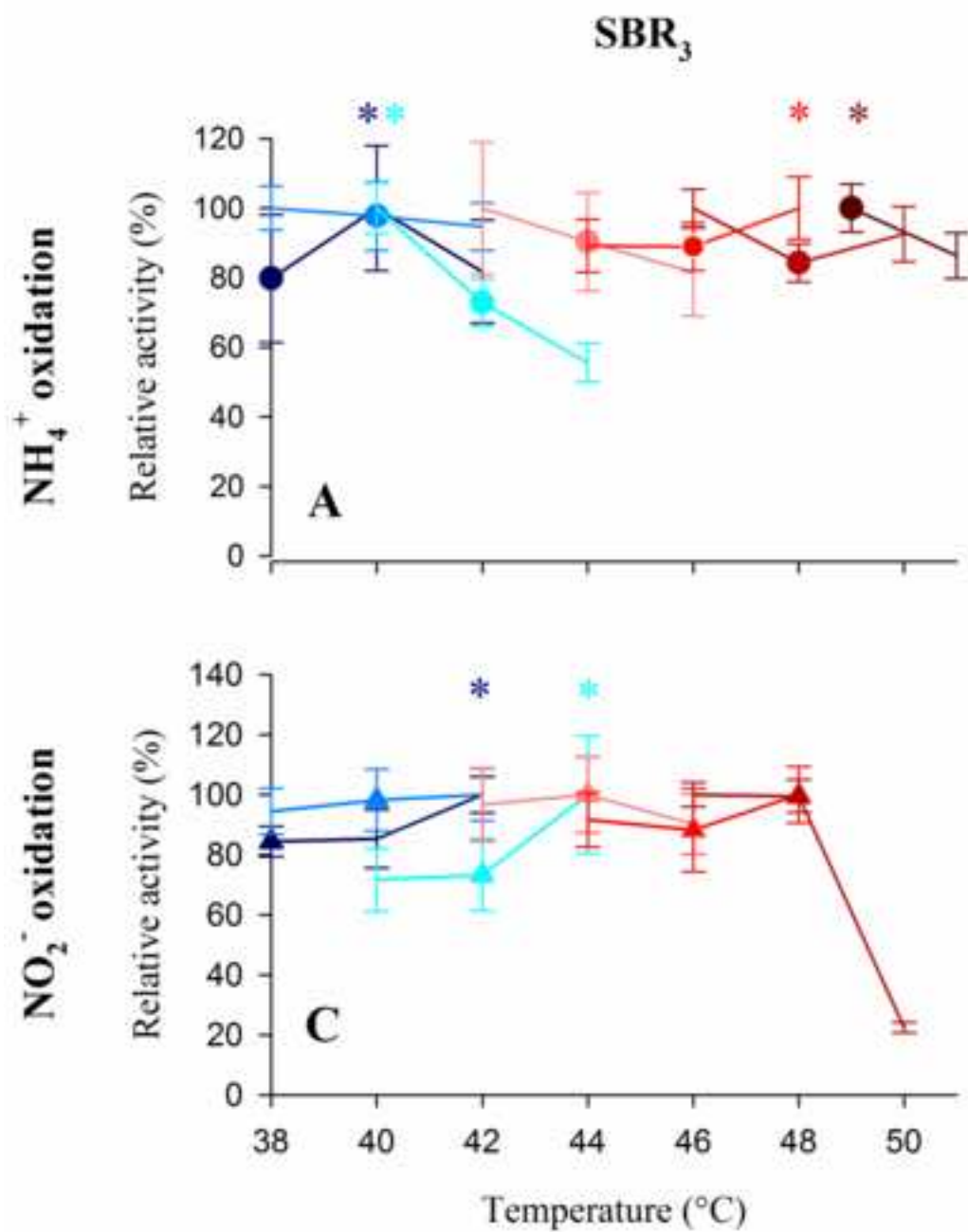


Figure 4

[Click here to download high resolution image](#)

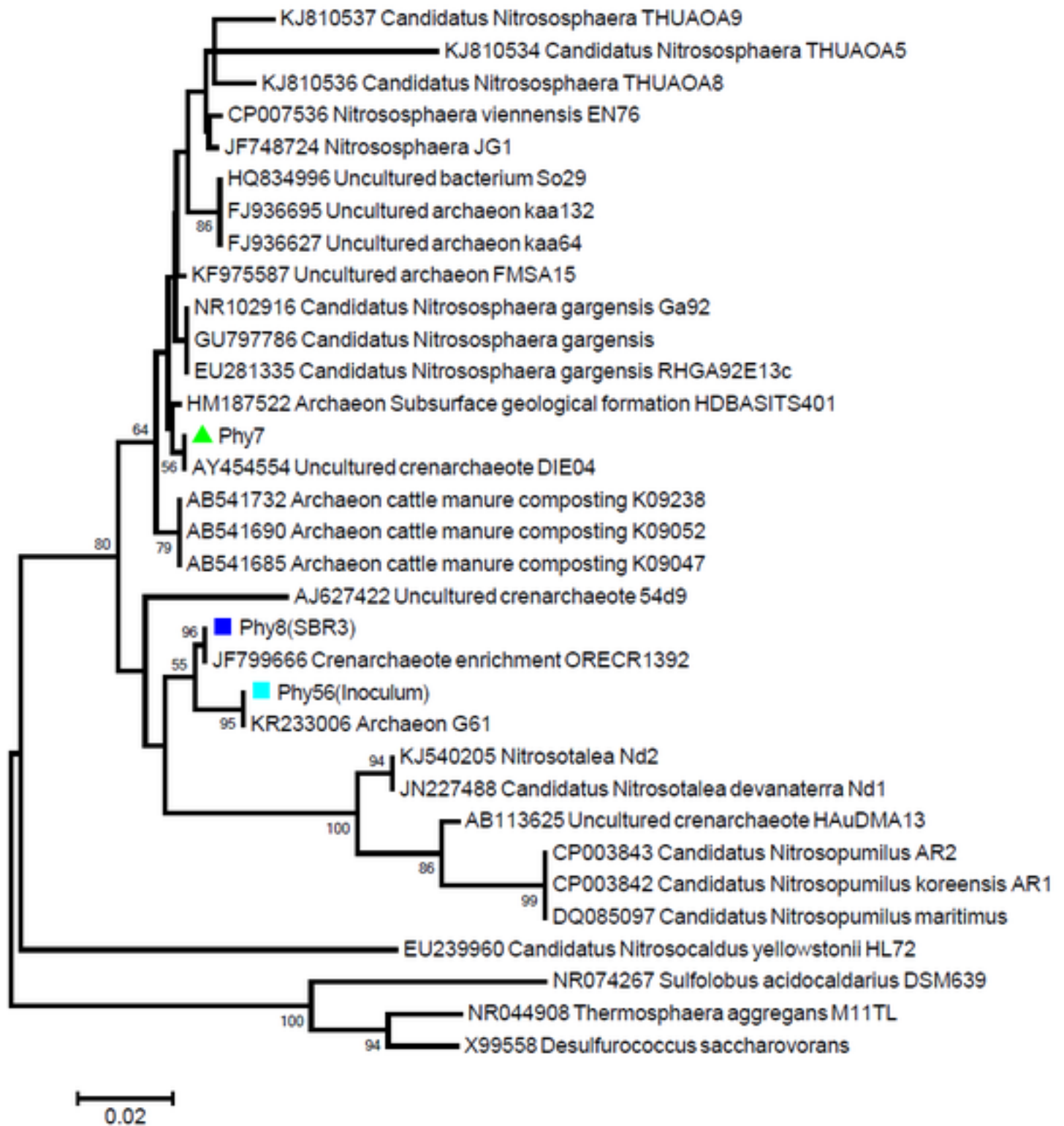


Figure 5  
[Click here to download high resolution image](#)

